Award Number: W81XWH-13-1-0099

TITLE: **A HYBRID NEUROMECHANICAL AMBULATORY ASSIST SYSTEM**

PRINCIPAL INVESTIGATOR: Ronald J Triolo, Ph.D.

CONTRACTING ORGANIZATION: Case Western Reserve University School Of Medicine
Cleveland OH 44106

REPORT DATE: June 2014

TYPE OF REPORT: Annual

PREPARED FOR: U.S. Army Medical Research and Materiel Command
Fort Detrick, Maryland 21702-5012

REPORT DOCUMENTATION PAGE

Form Approved
OMB No. 0704-0188

1. REPORT DATE	2. REPORT TYPE	3. DATES COVERED
June 2014	Annual	15 May 2013 – 15 May 2014

4. TITLE AND SUBTITLE
A Hybrid Neuromechanical Ambulatory Assist System

5a. CONTRACT NUMBER

5b. GRANT NUMBER
W81XWH-13-1-0099

5c. PROGRAM ELEMENT NUMBER

6. AUTHOR(S)
Ronald J Triolo, Ph.D., Rudi Kobetic, M.S.
Mark Nandor, M.S., Sarah Chang, B.S.

E-Mail: Ronald.triolo@case.edu

5d. PROJECT NUMBER

5e. TASK NUMBER

5f. WORK UNIT NUMBER

7. PERFORMING ORGANIZATION NAME(S) AND ADDRESS(ES)

Case Western Reserve University
10900 Euclid Avenue, Cleveland OH 44106

8. PERFORMING ORGANIZATION REPORT NUMBER

9. SPONSORING / MONITORING AGENCY NAME(S) AND ADDRESS(ES)
U.S. Army Medical Research and Materiel Command
Fort Detrick, Maryland 21702-5012

10. SPONSOR/MONITOR'S ACRONYM(S)

11. SPONSOR/MONITOR'S REPORT NUMBER(S)

12. DISTRIBUTION / AVAILABILITY STATEMENT
Approved for Public Release; Distribution Unlimited

13. SUPPLEMENTARY NOTES

14. ABSTRACT

A hybrid neuromechanical ambulatory assist system is being developed for walking after lower extremity paralysis that combines the stability and constraints of a novel hydraulic exoskeletal system with the mobility powered by the individual's own paralyzed muscles contracting via functional electrical stimulation. A mobile computing platform is designed to provide real-time closed-loop control using brace mounted sensors to deliver the stimulation needed to stand up and to move the body forward during walking while coordinating exoskeletal control mechanisms at the hips and knees to maintain stability. A hydraulic hip-knee coupling mechanism was designed to provide hip assisted knee flexion during early swing phase of gait to improve foot clearance. A variable constraint hip mechanism couples hips as needed to maintain posture and reduces the need for upper extremities to maintain balance. The knee locking mechanism is designed to allow the stimulated muscles to rest during stance while permitting unconstrained movement during swing. The exoskeleton is designed for easy fitting with adjustable uprights and hip abduction for donning for use in activities of daily living for persons with paraplegia.

15. SUBJECT TERMS
Exoskeleton, hydraulic, spinal cord injury, walking, rehabilitation, robotic

16. SECURITY CLASSIFICATION OF:			17. LIMITATION OF ABSTRACT	18. NUMBER OF PAGES	19a. NAME OF RESPONSIBLE PERSON
a. REPORT	b. ABSTRACT	c. THIS PAGE			USAMRMC
U	U	U	UU	40	19b. TELEPHONE NUMBER *(include area code)*

Table of Contents

Page

INTRODUCTION

The first prototype of the Hybrid Neuroprosthesis (HNP1) shown in **Figure 1** for walking in paraplegia was a combination of controllable exoskeleton, providing stability, and functional neuromuscular stimulation (FNS) of paralyzed muscles to power joint movements (Kobetic 2009). Hydraulic exoskeletal actuators were used to enable and disable joint constraints for transition through the gait cycle. The HNP1 incorporated two mechanisms for control of knees and hips – the Dual State Knee Mechanism (DSKM) which locked the knee for stance and unlocked it for swing (To *et al.,* 2011), and the Variable Constraint Hip Mechanism (VCHM) which locked the hip for stance, unlocked it for swing or reciprocally coupled the two hips to maintain posture (To *et al.,* 2008). A Variable Impedance Knee Mechanism (VIKM) using a magnetorheological (MR) damper was also tested as part of the HNP1 and shown to improve walking and stair descent (Bulea *et al.,* 2012, 2013). The HNP1 was controlled by an off board lab computer that read in the sensor data, determined phases of gait, applied the knee and hip joint constraints and modulated stimulation using a state based controller (To *et al.,* 2012, 2014). The evaluation in persons with paraplegia from SCI showed that walking with the HNP1 significantly reduced forward lean of FNS-only walking and the maximum upper extremity forces for balance and support by 42 % and 19% as compared to the isocentric reciprocal gait orthosis (IRGO) and FNS-only gait, respectively. The speed of walking with HNP1 was significantly faster than with IRGO and comparable to FNS-only with less stimulation, thus potentially reducing muscle fatigue. Drawbacks of HNP1 were weight of exoskeleton, lack of adjustability for fitting different users, limited knee flexion in early swing to provide proper toe clearance and being tethered to the laboratory-based computer, thus not conducive to evaluation in more realistic home and community environments. The purpose of this research is to prototype a HNP2 which will address these drawbacks and prepare it for evaluation outside of the laboratory.

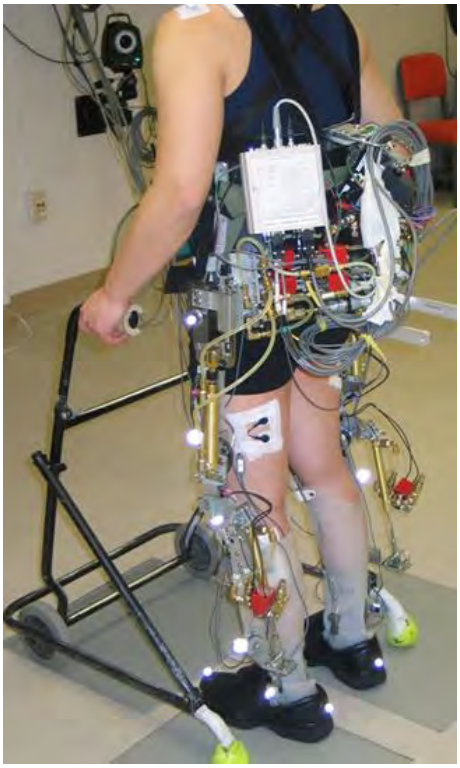

Figure 1. HNP1

BODY

Work Accomplished under Current Aims

Task 1 **– Design and implement new hydraulic hardware and control algorithms for synergistic coupling of hip and knee flexion during walking, including online adjustment of orthosis constraints and electrical stimulation.**

When using the HNP1, we were able to achieve sufficient hip flexion for use during swing phase of gait, but could not always achieve sufficient knee flexion especially in early swing. This resulted in

inconsistent and poor foot-floor clearance, which could lead to toe dragging and the inability to navigate uneven terrain. This motivated implementation of the hip-knee coupling (HKC) to improve toe clearance during early swing through coordinated hip-knee flexionStimulation driven hip flexion would enhance knee flexion through the coupling mechanism, thus decreasing the chance of toe dragging and increasing user safety during walking. Another advantage that hip-knee coupling should provide is to clear the lip of an upper step during stair ascent. Without sufficient knee flexion the leg gets caught on the lip and the user is unable to place the foot on the step above.

HKC Specification

Able-bodied hip and knee joint angles during gait at slow cadence were used to define HKC ratio of the hydraulic circuit (Winter 1991). The able-bodied hip angle vs. knee angle were plotted to determine the relationship between the two joints during gait (**Figure**, red shapes). The initial portion of swing phase was analyzed to calculate the hip-knee joint angle ratio (**Figure**, blue shapes with linear trend line). During pre- and early-swing the hip:knee ratio is approximately 0.43°:1° (or 1°:2.3°).

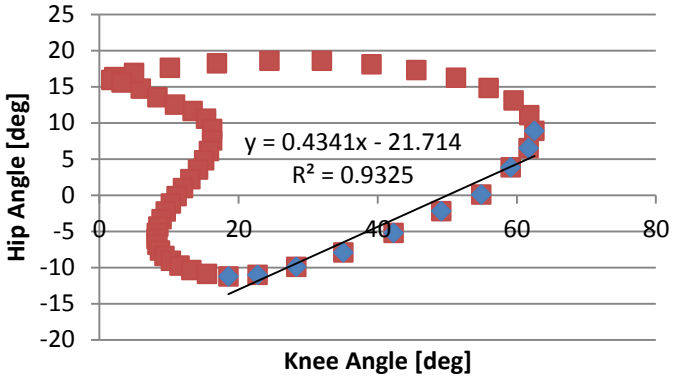

Figure 2. Hip-knee angle for slow able-bodied gait.

HKC Design

An initial HKC hydraulic mechanism (**Figure**) was designed, fabricated, and incorporated into the current HNP1 hardware that coordinated flexion of the hip and knee joints during swing phase, where hip flexion aided knee flexion. The hydraulic circuit for the right leg has the states of hip independently free or locked, knee independently free or locked, and hip-knee coupled. The HNP1 with variable constraint hip mechanism (VCHM) and dual state knee mechanism (DSKM) were modified to incorporate the hydraulic HKC mechanism which includes the connections between rod side of the hip cylinder and rod side of the knee cylinder (as well as blind side of the hip cylinder and blind side of the knee cylinder), and the addition of valves to create the additional HKC states. Hip and knee hydraulic cylinders were selected such that the volume ratio of the two cylinders' rod sides achieved the approximate 1°:2.3° hip-knee ratio, according to the following equation:

$$\frac{volume_{hip}}{volume_{knee}} = \frac{\pi * \left(\frac{bore^2}{4}\right) * stroke}{\pi * \left(\frac{bore^2}{4}\right) * stroke} \approx 2.3$$

Components used in this unilateral HKC hydraulic circuit are listed in **Table 11**. The ratio achieved by the 7/8" bore hip cylinder and 9/16" bore knee cylinders is 1°:2.4°, where

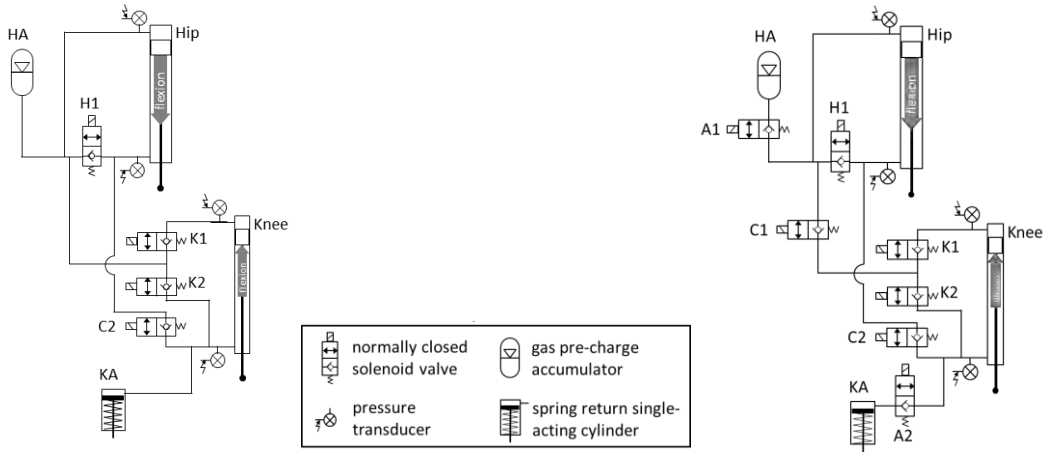

Figure 3. HKC Hydraulic Circuit for the right side, version #1 (left) and version #2 (right)

$$\frac{volume_{hip}}{volume_{knee}} = \frac{\pi*\left(\frac{0.875^2}{4}\right)*3}{\pi*\left(\frac{0.5625^2}{4}\right)*3} \approx 2.4$$

The first version of the HKC hydraulic circuit (**Figure** , left) did not function as expected. The hip-knee coupling ratio was inconsistent, and movement of the hip cylinder did not always result in a proportional movement of the knee cylinder. In this circuit, the fluid still has access to the knee and hip accumulators, which is providing a unintentional destination for fluid intended pass only between the cylinders. The HKC hydraulic circuit was improved by adding the ability to block flow to both accumulators (valves C1, A1, and, A2 in **Figure** , right) and ensure that fluid was not moving to the knee when the joints were functioning independently.

Table 1. Unilateral HKC Mechanism Hydraulic Components

	hip cylinder	**knee cylinder**	**valve**	**hip accumulator**	**knee accumulator**
manufacturer	Clippard Minimatic	Clippard Minimatic	Allenair	Hydac	Clippard Minimatic
type	double acting	double acting	solenoid 2/2	gas pre-charge (58 psi) diaphragm	single acting spring return
bore	7/8”	9/16”	-	-	3/4”
port	1/16” NPT	1/16” NPT	1/8” NPT		1/8” NPT
orifice	-	-	2.38 mm	-	-
stroke	3”	3”	-	-	1”
rod diameter	0.25”	0.25”	-	-	0.25”
Size	-	-	-	0.075 L	
voltage	-	-	12 VDC	-	-
power consumption	-	-	7 W	-	-
C_V	-	-	0.176 B → A 0.166 A → B	-	-
response time (no load)	-	-	12 ms (on) 43 ms (off)	-	-
max operating pressure	2000 psi	2000 psi	-	3600 psi	250 psi
spring force	-	-	-	-	3 lbs installed 6 lbs compressed
cracking pressure	-	-	46 ± 7 psi	-	-

Version #2 of the HKC hydraulic circuit was bench tested to determine (1) the passive resistance due to the hydraulics and (2) the coupling ratio of the hip-knee joint coupling. The system was pressurized to approximately 70 psi to minimize compliance due to any remaining air bubbles in the circuitry. The hydraulic HKC mechanism was attached to the uprights on the right side of the exoskeleton of the HNP1 and affixed to the Biodex robotic dynamometer (Biodex Medical Systems Inc., Shirley, NY, USA) arm as shown in **Figure 4**. The dynamometer measured the joint angle, angular velocity, and torque of the hip joint. The dynamometer arm was set in passive mode and passive resistance was measured at constant angular velocities from 30 °/sec to 180 °/sec in 30 °/sec increments. Hip and knee joints were instrumented with linear and rotary potentiometers (Vishay Spectrol, Malvern, PA, USA), respectively.

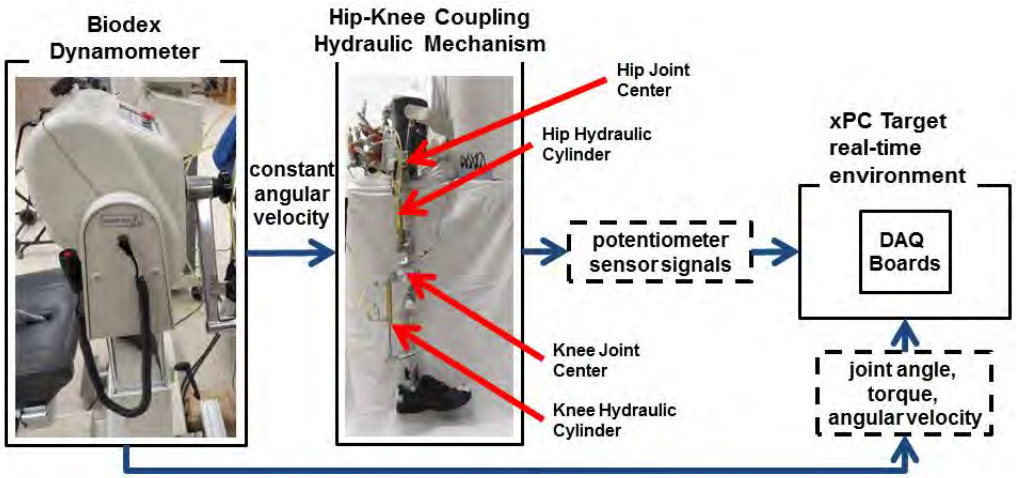

Figure 4. Experimental setup with Biodex dynamometer.

All dynamometer and potentiometer data were collected at 200 Hz and filtered online with a 5^{th} –order low-pass digital Butterworth filter with a cutoff frequency of 10 Hz. The pressure data were filtered online with a 7^{th} –order low-pass digital Butterworth filter with a cutoff frequency of 20 Hz. The dynamometer and angle data were filtered offline with a 5^{th} –order low-pass digital Butterworth filter with a cutoff frequency of 3 Hz and 40 Hz, respectively.

HKC Bench Test Results

Passive resistance is the torque needed to move the system at a specific angular velocity when the hip or knee joints of the HKC mechanism (Version #2) are in a freed or coupled state. The average passive resistance of the hip measured at 30° of flexion when the joint is flexing (negative) and extending (positive) when the hip joint is moving independently at increasing angular velocities is shown in Error! Reference source not found.**a,** and when the hip and knee are coupled in Error! Reference source not found.. The maximum angular velocity during able-bodied gait occurs near a knee flexion angle of 30°. Because passive resistance is proportional to angular velocity, the largest amount of passive resistance should occur at the knee angle of 30°.

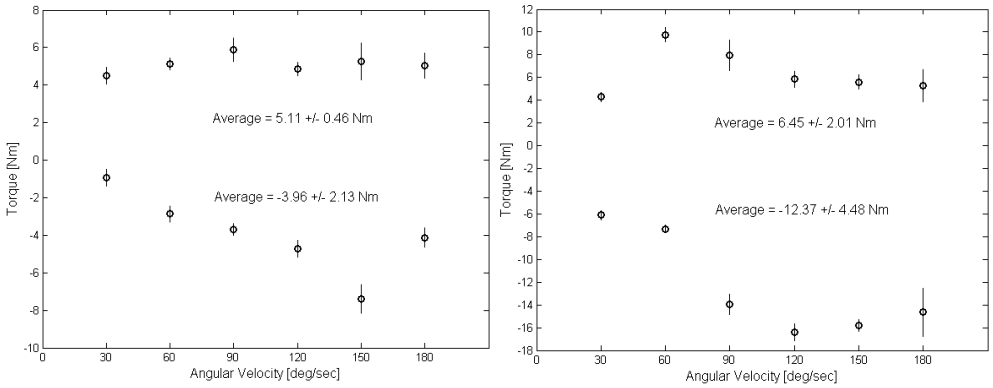

Figure 5. Passive resistance of the hip at 30° of flexion when **a)** the hip is independently flexing (negative) and extending (positive) and **b)** when the hip is flexing and extending with HKC active.

The average passive resistances at the hip joint listed in **Table 2** were determined by averaging all passive resistance values over all angular velocities.

Table 2. Average Passive Resistance at Hip Joint

Movement	Hip Independent	Hip-Knee Coupling
Extension	5.11 ± 0.46 Nm	6.45 ± 2.01 Nm
Flexion	-3.96 ± 2.13 Nm	-12.37 ± 4.48 Nm

The passive resistance generally increases as a function of angular velocity up to 90°/sec and then levels off at 3.70 ± 0.31 Nm when the hip is independently moving in flexion. The increase in passive resistance is greater when hip and knee are coupled and levels off at an average of 7.93 ± 1.33 Nm when extending and 13.7 ± 0.87 Nm when flexing at an angular velocity of 90 °/sec. Positive torque indicates resistance to extension, and negative torque indicates resistance to flexion.

The average passive resistance at the knee measured at 30° of flexion when flexing (positive) and extending (negative) when the knee joint is moving independently is shown in Error! Reference source not found. and the average passive resistance values for the different constant angular velocities are shown in
Table 3.

Table 3. Average Passive Resistance at Knee Joint

Movement	Knee Independent
Flexion	4.06 ± 0.78 Nm
Extension	-2.72 ± 0.57 Nm

Coupling ratios between the hip and knee joint angles were analyzed to determine the knee joint flexion angle that is assisted by ipsilateral hip joint flexion (

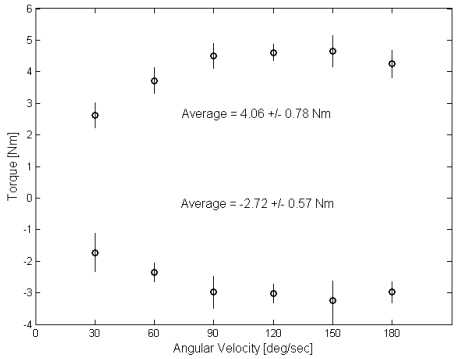

Figure 6. Passive resistance at 30° of knee flexion when moving independently in flexion (positive) and extension (negative).

Table 4 and
Table 5). The joint angles were determined from the linear and rotary potentiometers instrumented at the hip and knee joints, respectively, during constant angular velocity with the HKC mechanism coupled. The average hip-knee coupling ratio was calculated by two methods: (a) calculating the slope of the hip-knee plot at each joint angle (*i.e.* , time point or index value) and averaging all of these slopes together (
Table 4) and (b) fitting a line to the overall hip-knee angle plot (
Figure) only during regions of constant angular velocity and averaging the slopes of the fitted lines (
Table 5). An example of the hip-knee movement is shown in
Figure .

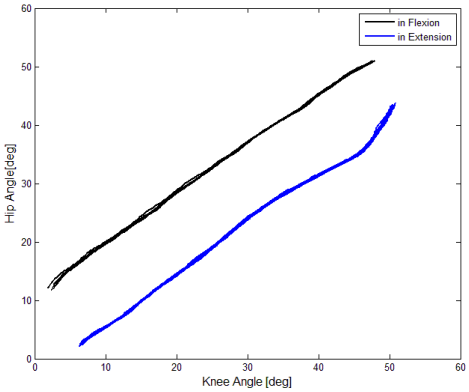

Figure 7. Example hip and knee movement during a constant angular velocity of 60 °/s.

Table 4. The average HKC ratio by finding the ratio at each time point (Method a).

Angular Velocity	30 °/sec	60 °/sec	90 °/sec	120 °/sec	150 °/sec	180 °/sec
HKC ratio In Flexion	1.03 ± 0.48	1.14 ± 0.23	1.22 ± 0.28	1.28 ± 0.21	1.41 ± 0.18	1.52 ± 0.17
HKC ratio In Extension	1.08 ± 4.62	1.08 ± 0.35	1.07 ± 0.41	1.11 ± 0.45	0.85 ± 0.24	1.07 ± 0.33

Table 5. The average HKC ratio by fitting a line to the hip-knee angle data during constant angular velocity (Method b).

Angular Velocity	30 °/sec	60 °/sec	90 °/sec	120 °/sec	150 °/sec	180 °/sec
HKC ratio In Flexion	1.11 ± 0.87	0.97 ± 0.33	0.88 ± 0.02	0.80 ± 0.03	0.72 ± 0.04	0.66 ± 0.09
HKC ration In Extension	0.67 ± 1.19	0.87±0.003	0.84 ± 0.01	0.87 ± 0.04	1.24 ± 0.28	0.99 ± 0.27

The HKC ratio was estimated for a particular hip flexion angle (e.g., 30° of hip flexion) by fitting a linear polynomial to the data over a window starting from three degrees before the target angle and ending at three degrees after the target angle. Each constant angular velocity trial had multiple repetitions, which resulted in several HKC ratios from fitting a line at each 30° of hip flexion angle. The slopes from the linear fit of the target angle were averaged together within the constant angular velocity portion of the trials to find the average HKC ratio for that particular hip flexion angle (**Table 6**).

Table 6. The average HKC ratio at 30° by fitting a line about a specific target value of hip flexion angle

Hip Angular Velocity	30 °/sec	60 °/sec	90 °/sec	120 °/sec	150 °/sec	180 °/sec
HKC ratio	1.24 ± 0.04	1.14 ± 0.04	1.05 ± 0.09	1.28 ± 0.07	*	*

*does not consistently reach 30° of hip flexion during that particular constant angular velocity

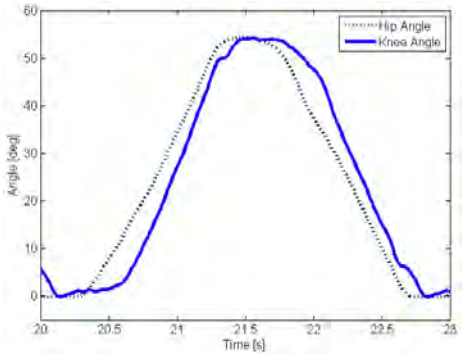

Figure 8. Example hip and knee angles at 60 °/sec demonstrating time delay.

Coupling delay is the time between the start of hip flexion and the beginning of ipsilateral knee flexion with hip-knee coupling engaged (**Figure**). The delays for the different constant angular velocities are shown in

Table 7.

Table 7. Hip-Knee Coupling Delay [ms]

Angular velocity	30 °/sec	60 °/sec	90 °/sec	120 °/sec	150 °/sec	180 °/sec
Delay during flexion	*	136 ± 29	15.6 ± 9.6	47.5 ± 12.3	4.3 ± 0.57	9.1 ± 0.73

In addition to the time delay, there was an increase in offset of knee angle as the angular velocity increased (**Figure 9)**. The reason for this behavior is being investigated, and might be due to compliance in the system, either mechanical compliance or compliance due to residual air in the hydraulic circuit.

HKC Mechanism Discussion

The passive resistance increased with HKC as compared to independent movements of the hip or knee joints. Approximately 23% of the hip flexion torque generated by FNS would be needed to overcome the passive resistance during coupling (Kobetic 1994). An effort is underway to identify and address the inconsistent hip-knee coupling ratios and identify and minimize the source of passive resistance.

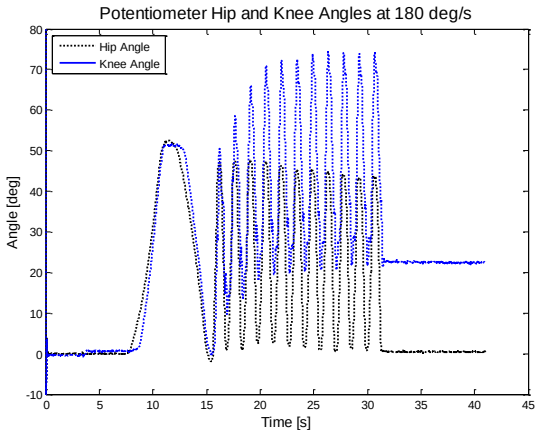

Figure 9. Offset in knee angle observed at higher angular velocities

In general, the hip-knee coupling ratio is slightly over 1 and shows a slight increase with increasing angular velocity (
Table 4 and
Table 5). The variance in hip-knee coupling ratios may be due to compliance in the system. There is mechanical compliance in the rack and pinion gear used at the hip joint on the exoskeleton, and any residual air in the hydraulic system could also create compliance. The valves used in the hydraulic circuit can be a potential cause for the inconsistent ratio between the hip and knee joint angles. Because the cracking pressure for the valves is relatively low at 46±7psi, fluid could flow through these check valves if that pressure is exceeded (ex. valves H1 or K2). Experiments are underway that measure rod and blind side cylinder pressures to see whether these pressures are being exceeded.

Normative able-bodied data during gait show an approximate 1:2 ratio between the hip and knee joint angles in flexion (Winter 1991). According to cylinder volumes, the ratio should be 2.4. The preliminary

results for the HKC hydraulic mechanism have an average hip-knee coupling ratio ranging between 1.03 and 1.52. This difference could be due to difference in linear to rotary transmissions at the hip and knee and is also being investigated.

The hip-knee coupling ratio at 30° of hip flexion is approximately 1 for constant angular velocities ranging from 30°/sec to 120°/sec. The ratio stays relatively constant at this particular hip flexion angle, even as the angular velocity increases. It was difficult to find the ratio values for the higher angular velocities (150 and 180 °/sec) because the hip flexion angle did not consistently reach 30°.

The time delay does not hinder the ability of the mechanism to create coupling between the hip and knee joints, but it does influence the resulting coupling ratio. Knee flexion does not start immediately upon initiating hip flexion. After a short time delay, the knee begins to flex in response to the flexing hip. Implementing the HKC mechanism during gait may require planning for this time delay to ensure that sufficient knee flexion angle is reached to clear the foot during early swing. Efforts are also underway to minimize this delay.

Up to date results shows that hip-knee coupling using a hydraulic mechanism can be achieved. Testing is underway to get a better understanding of variability in hip-knee coupling ratio, knee flexion delay and the source of passive resistance. Continuing this work will involve incorporating HKC into the state based controller developed for HNP1 and determining how the HKC ratios created by the hydraulics affect the foot-floor clearance during swing phase of gait.

Task 2 – Refine the design of the currently existing hybrid neuroprosthesis (HNP1) prototype orthosis and hydraulic system to minimize size, weight, enable rapid fitting, and provide easy donning and doffing in the field.

HNP1 was designed as a proof-of-concept using existing off-the-shelf hydraulic and orthotic components. In the first year of this project a considerable effort was dedicated to designing, manufacturing and testing hydraulic components to minimize size and weight of the exoskeleton for HNP2. Additional effort was exerted tp redesign the supporting structure of the exoskeleton for mounting of hydraulic components and to enable easy fitting and donning by the user.

Design Input Requirements – Specifications were set for an intended user with a maximal weight limit of 100kg and anthropomorphic measurements spanning from the 5th percentile female at the low end to the 95th percentile male at the high end, based on data from the National Health and Nutrition Examination Survey (NHANES). The measurements pertinent to the exoskeleton design are included in **Table 8**.

Table 8. Anthropomorphic data

Measurement	Exoskeletal part	5th percentile female (in)	95th percentile male (in)

Floor to lateral femoral epicondyle	Leg upright	16.4	21.7
Lateral femoral epicondyle to greater trochanter	Thigh upright	14.3	18.4
Hip breadth	Corset/thoracic jacket	11.3	14.2

Joint Torque Specification

Knee torque requirements - The torque requirements for the knee are presented in the form of a graph of torque vs. knee angle shown in **Figure 10**. In this graph, negative angles indicating knee flexion, positive indicating hyperextension. The torque shown in the graph is the maximum resistive torque that is required at specified angles (positive for hyperextension, negative for flexion) for most activities of daily living. Technical specifications are based on a 100 kg (220 lb) user.

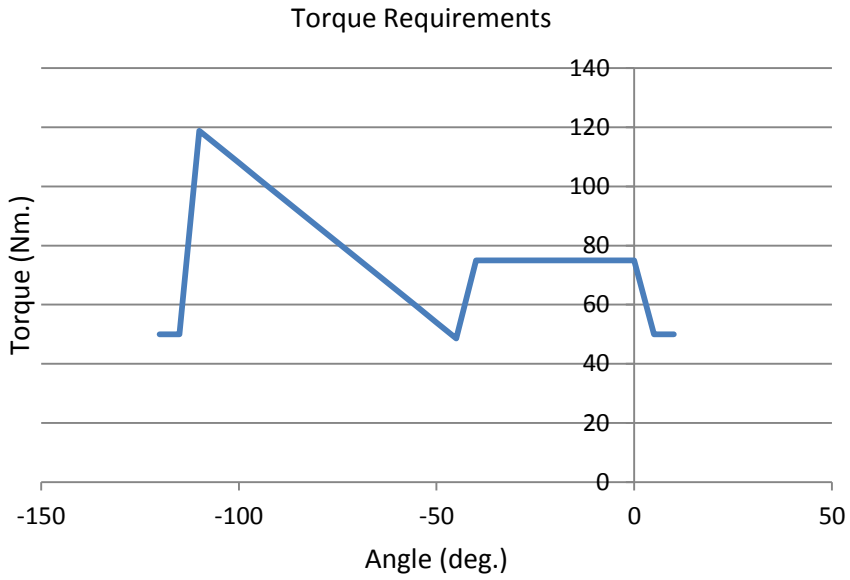

Figure 10. Resistive knee moment requirements for most activities of daily living

Knee at 0° to 10° of hyperextension - In this region, because of the hyperextension, the knee is statically stable as long as the gravitational vector of the center of mass is projected in front of the knee. Thus, a 50 Nm constant torque was specified as adequate.

Knee at 0° to 40° of flexion - During testing of the HNP1, loading response during gait took place over an angular range of full extension to approximately 25° of flexion. To provide an additional margin of safety, the design specification range was extended to 40° of flexion. The maximum damper torque utilized during evaluation of the HNP1 with a MR damper controlling the knee combined with quadriceps stimulation during gait was 47 Nm, with a 63 kg user (Bulea *et al.* 2012). Linearly scaling up for a 100 kg user yields a torque requirement of 75 Nm.

Knee at 40° to 110° of flexion - This region of linearly increasing torque is based on data collected from able bodied individuals performing stand to sit maneuvers. The slope of the line is approximately .0108 [Nm/kg]/ degree translated into torque values for a 100 kg user.

This is also the range of knee angles during stair descent with torques of 1.55 Nm/kg for able bodied subjects (2). From a technical standpoint, the device size to achieve this torque would be big and bulky. To keep device size reasonable, able bodied stair climbing will not be used as a benchmark, but data published on other exoskeletons which report 0.35 Nm/kg (3). For a 100 kg subject, that translates into 35 Nm of torque which is below the requirements stated above thus significantly reducing the upper extremity effort needed for support.

Knee at 110° to 120° of flexion - This angular range is provided more for user comfort and ease of storing, donning, and doffing, thus the torque requirements were reduced to 50 Nm.

Hip torque requirements - Unlike the knee joint, which is primarily used in both support (locked) and energy dissipation (damped) modes, the hip joints are primarily used for support and potentially power assist functions. Thus, required toques for the hip are much lower than the knee as shown in **Figure 11** and were determined under following considerations:

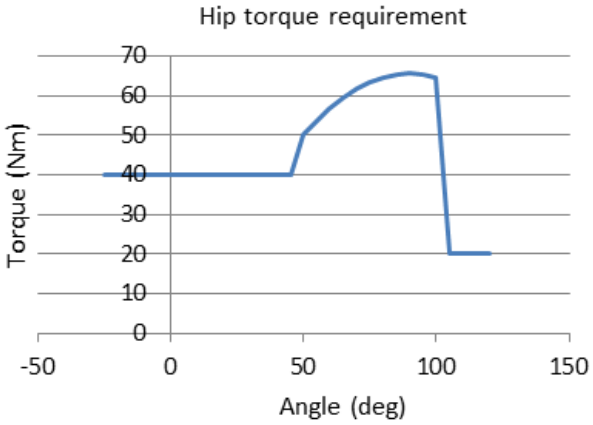

Figure 11. Hip torque requirements.

1) Torque for hip hyperextension (negative) to 45° of flexion (positive) encountered during walking. The HNP1 hip joints were designed to lock against an applied torque of 35 Nm, this value being the maximum value determined during an experiment with a subject with SCI utilizing both FNS and a conventional RGO. During evaluation of the HNP1, actual joint torque did not exceed 15 Nm (To *et al.* 2010). However, this static locking torque is increased to 0.4 Nm/kg (Winter 1991) or 40 Nm for a 100kg subject.
2) Torque for hip flexion from 45° to 105° encountered during a high step was determined by calculating the necessary torque to be able to lift the user's leg and the attached brace for the purpose of climbing stairs.
3) Torque for hip flexion greater than 100° was specified for device comfort and usability.

Transmission Options and Evaluation

A number of transmission options were evaluated for HNP2.

Rack and pinion gear set - This arrangement was incorporated at the hip joint in HNP1, with the rack attached to the cylinder, and the pinion attached to the joint. It was tested to 70 Nm of applied torque. The advantages of this transmission arrangement include its simple design, and constant moment arm

and torque profile throughout the range of motion. The limiting factor in this transmission is the gear material yield strength. The disadvantages are weight, mechanical compliance or backlash, and possible bending moments of the cylinder rod.

3-bar linkage - This arrangement was incorporated at the knee joint in the HNP1 with a 9/16" bore cylinder. Advantages are the simplicity of the design design, ease of fabrication, low weight (especially important at distal joints), low compliance, and a linkage arrangement that can be shaped to maximize torque in specific range of joint movement. Disadvantages include moment arm and torque profile that varies with joint angle, and potential singularities and points of zero moment holding capability (as in HNP1 at 75° of knee flexion).
Because of the many advantages offered by this transmission it is being incorporated in the exoskeleton of the HNP2. Their respective attachment points to the uprights and the resulting torque profiles are presented in detail in **Appendix A**.

Rotary actuator – This option was not considered for the HNP1 because commercially available devices are significantly heavier compared to traditional linear cylinders. However, the hip-knee coupling capability of the HNP2 requires equal fluid volume exchange between hip and knee actuators, or the addition of accumulators. A rotary actuator with equal fluid displacement on both sides of the sealed surface would eliminate the need for accumulators. Additional benefits of rotary actuators are the significant decreases in overall part count, complexity, and weight. Furthermore, because rotary actuators naturally produce rotary motion, the need for transmissions is eliminated. While the prototype actuator we developed is heavier than a comparable linear cylinder, elimination of the transmission components as well as the necessary accumulators would reduce the overall weight of a system utilizing rotary actuators.

A rotary actuator was designed, prototyped and bench tested for possible use in HNP2. This work is described in **Appendix B**. In summary, the actuator consists of a 6061-T6 aluminum case and vane, utilizing rubber seals riding grooves cut in the vane to positively seal against leaking hydraulic fluid. Evaluation and testing revealed that the seal design needs further work, resulting in a maximum 100% sealing pressure of only 20 psi, and a rather high passive resistance of 12 Nm. Both of these deficiencies would require a major effort in redesign and fabrication which is beyond the scope of this study. Thus, it was decided to modify the hydraulic mechanisms and transmission of the HNP1 with off the shelf components and defer further pursuit of a custom rotary actuator design.

Hydraulic Circuitry and Evaluation

Valve Assessment

An assessment of hydraulic valves was made in an effort to reduce the size and weight of hydraulic circuitry in HNP2. In the HNP1, 2 way, 2 position valves from Allenair, in both normally closed (NC) and normally open (NO) configurations, were used. A total of eight valves were required for HNP1 including

one in each DSKM, and six in the VCHM. To create the additional hip-knee coupling states, 14 valves would be needed if the same valves were utilized.

Cartridge valves - An alternative to the Allenair valves are cartridge valves. While individual valves are larger than the Allenair valves, they offer several advantages. First, industrial cartridge valves are available in more complex configurations than the Allenair valves, meaning that a single solenoid can control three, four, or six individual ports. Using this property, all the necessary states to create the HNP2 can be achieved with only seven 4 way, 2 position valves. Second, these valves are designed with o –ring seals and threaded shafts so they can be placed in specially designed hydraulic manifolds. While individual manifolds are available, the real advantage is the possibility of creating a single manifold to hold multiple valves, thus reducing the size and weight.

High speed valves – We explored the option of utilizing a high speed solenoid valve connected between the ports of a cylinder to regulate flow and to provide a measure of damping at the knee, a function useful to controlling knee flexion during loading response and weight acceptance during gait, as well as during for the stand-to-sit maneuver and stair descent. We hypothesized that any vibrations caused by closing and opening of the valve at speeds would be filtered by the inertia of the system, resulting in smooth controlled displacement of the cylinder and output motion at the knee. We tested a commercially available high speed valve from Clean Air Power for this application as described in **Appendix C**. As a damper, the valve could only operate at low frequencies (10 Hz), where the valve has enough time to close. However the resulting motion at that frequency was unacceptably jittery. The valve is not designed to work in the configuration proposed for knee damping as desired for HNP2. Specifically, it is clear from the test results that not having the necessary high pressure supply to return the valve to its closed position resulted in unacceptably slow valve closure times.

Prototype servo based proportional valve - In the absence of commercially available industrial valves that provide sufficient resolution, a prototype proportional valve was designed, prototyped, and tested as described in **Appendix D**. The results indicates that there is too much leakage in the valve to be suitable for use in a knee damping mechanism. At 200 psi the valve allowed 0.86 gpm of fluid to pass in its closed configuration, which is significantly higher than the specified flow (0.3 to 0.7 gpm) for the knee mechanism. While this remains a potentially attractive solution to the problem, given limited time and resources this option is beyond the scope of this research project and further development of custom valves was deferred.

Manifold Options - In the HNP1 brass connections were used to interconnect hydraulic valves. For the HNP2, manifolds were explored as an alternative to connecting hydraulic valves with connectors and tubing in an effort to save space, reduce potential for leakage, reduce resistance to flow and to create a cleaner appearance.

A manifold that is integrated into the femoral upright of the HNP2 was considered initially (**Figure 12**). This design offers many advantages in terms of clean packaging by eliminating most of the tubing and integrating the necessary valves and actuators into a single pieces.

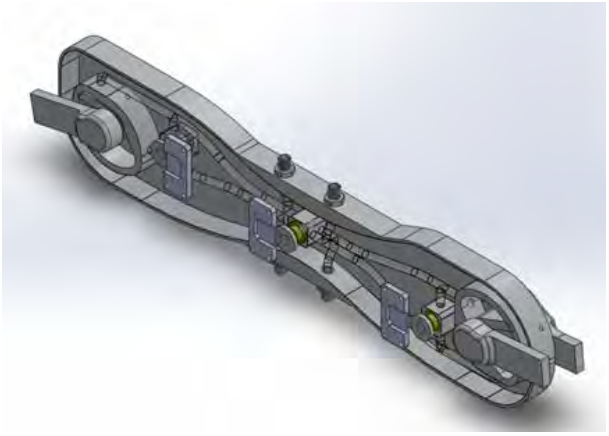

Figure 12. Integrated rotary actuators and manifold.

The disadvantages of this design are:

- difficult to make it adjustable length for fitting
- relies on rotary actuators since it requires the actuators to maintain their orientation and spacing with respect to each other.

Because of these disadvantages this design was deferred for use in HNP2.

A more flexible arrangement places all the necessary hydraulic valves, accumulators, and pressure sensors on the back of the corset (**Figure 13**). In this arrangement, the uprights are simply carrying the cylinders while the corset-mounted manifold houses the cartridge valves. Although this increases the number of hydraulic lines running to each upright compared to **Figure 12**, they can be hidden within appropriate shielding and covers. More importantly, this approach locates most of the heavy components off the uprights, decreasing the torque necessary from stimulation to overcome the weight of the device.

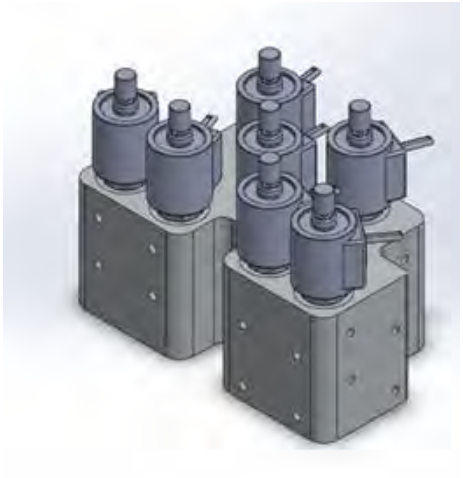

Figure 13. Manifold for cartridge valves.

Given the overall complexity of the hydraulic circuit, it may not be possible to assemble all valves into a single manifold. It may be preferable to package the left side, the right side, and the center/accumulator into separate manifolds. Once the hydraulic circuit is finalized the packaging and manifold will be addressed with a design that balances the number of fittings and overall size with complexity and physical realization.

Supporting Structure of the Exoskeleton

The mechanical design of the supporting structure of the exoskeleton for HNP2 aims to integrate all the subsystems into a complete package that is safe, functional, lighter and easier to assemble/dissemble than the prior system. This will be accomplished through the use to manufacturing techniques that were not a viable option during design and construction of the structure for HNP1. Currently there are a number of manufacturing options available. These include:

1) In-house machining capability consisting manually operated mills and lathes, as well as 3-axis CNC mill and 2-axis CNC lathe. If additional capability is needed, local manufacturers with 4- and 5-axis mills are available.
2) In house 3-D printing (Rapid Prototyping) capability. Polymer additive manufacturing has become much more prevalent and affordable in recent years, and a new 3-D printer has been acquired to augment the several devices available on campus at CWRU and enhance our in-house manufacturing capability.
3) Outside vendors and shops. In addition to our in-house capability, outside vendors will be utilized for specialized processes such as 2-D CNC water jet or CNC laser cutting, which are able to quickly and easily making parts from .25" or .375" aluminum pieces.

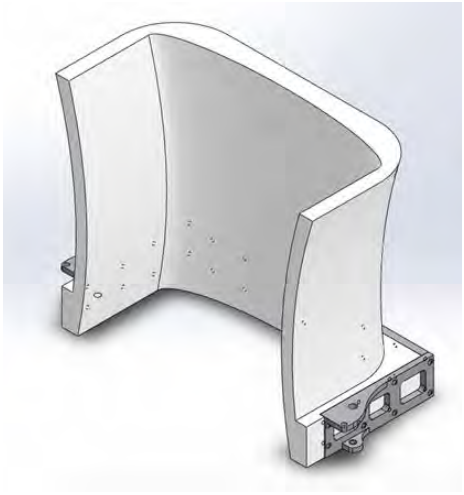

Figure 14. Corset

The structural components of the exoskeleton include: corset, thigh upright, shank upright, and footplate/AFO. Each subsystem will be evaluated individually.

Corset - The corset/thoracic jacket provides trunk support and stabilizes the pelvis, is a mounting structure for the manifold, hydraulic valves, control electronics, and batteries, locates the hip center of rotation, and serves as a mounting point for the femoral uprights. The standard corset used in RGOs and adapted for HNP1 offered limited flexibility from a mechanical design perspective, particularly due to the difficulty of mounting components on it. To overcome this, a higher degree of customization is required. A structural frame of three different sizes (small, medium and large) will be used for attaching hydraulic components posteriorly and the custom fitted corset anteriorly. The frame will also provide attachment for the thigh upright. A custom fit thoracic-lumbo-sacral orthothis (TLSO) will be fabricated for each user, either via traditional vacuum forming techniques or additive manufacturing/3D printing, and mounted within the frame. This design allows metal parts to be easily added to the corset, while maintaining mechanical strength and stiffness by tying together the left and right upright femoral upright attachment points.

Thigh upright – Critical points to consider for the thigh components are: attachment to the corset, hip abduction joint for ease of donning and doffing, upper and lower cylinder attachment points, joint position sensors, and length adjustment. According to the design specifications, this section must be adjustable between the 5^{th} percentile female and 95^{th} percentile male (14 inches to 18 inches).

Many different options were considered to making this structure adjustable, including telescoping tubing of varying cross sections, grooved junctions, etc. The solution shown in **Figure 15**, which locates the hydraulic pistons between two structural members was chosen for the following reasons:

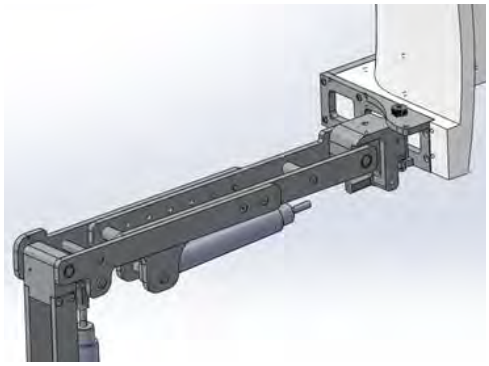

Figure 16. Thigh abduction for donning and doffing while sitting.

1) The double upright structure solution reduces the bending moment placed on the cylinder by fully caging it on both sides. The truss like structure also reduces bending moments on the upright.

2) The solution is easy to manufacture – by using .25" 6061-T6 aluminum, and keeping a 2-D profile, these pieces can be easily water jet or laser cut.

3) Because it is easily manufactured, it is easily modified. For example, modifying linkage pickup points, modifying to accept a different size cylinder (i.e. larger hip cylinder to try different coupling ratios) are a quickly redesigned and refabricated with this arrangement.

Internal spacers guarantee rigidity between the two adjustable pieces, and the actual adjustment is accomplished by removing 4 button head cap screws, adjusting to correct length, and replacing screws.

The thigh upright contains a hip abduction joint necessary for ease of donning and doffing of the device. This is performed by removing the T-handle pin and swinging out the upright, as illustrated in **Figure 16**. Rotation of the device is performed around a shoulder bolt. To ensure safety, the shoulder bolt is help in place with a nylock nut. To ensure smooth rotation, all bearing surfaces ride on oil-lite bronze bushings. Joint position will be measured by absolute digital encoders from US Digital (MAE3 magnetic encoders). These encoders can either report joint angle as an analog signal or a PWM signal, with duty cycle corresponding to angular position.

Shank Upright - Continuing distally is the shank upright, similar in construction to the femoral upright, fully encaging the cylinder to reduce bending loads and designed for ease of manufacture. Instead of layering a second layer of aluminum to get the necessary adjustability, a series of holes can provide the necessary functionality without the weight or complexity of more pieces as shown in complete assembly in **Figure 17**. Those holes are meant to connect to whatever footplate or ankle foot orthoses (AFO) are desired. In the spirit of flexibility, the choice of foot attachment and interface has not been directly specified, and the bolt pattern is intended to accept multiple designs for evaluation and testing purposes. These holes are offset 1 inch to the rear to mimic previous work. Additionally, further adjustability can be found in the sizing of the foot interface pieces.

Future CAD work will add safety shields and covers to eliminate pinch points, provide a barrier against oil spills, and to provide a cleaner, more cosmetic appearance.

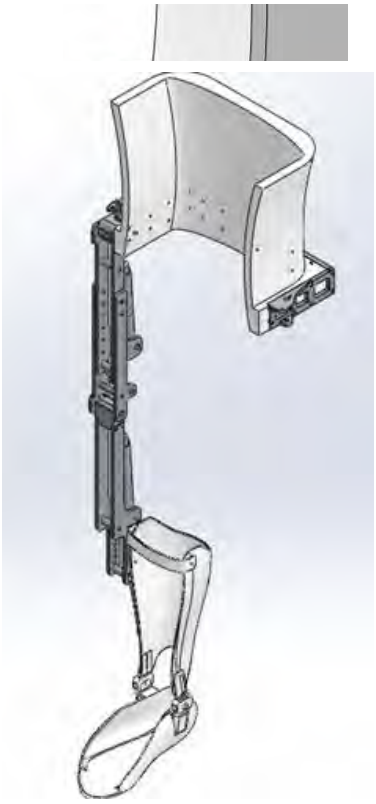

Figure 17. CAD drawing of the right side exoskeletal assembly.

Task 3 – **Design, develop and implement a new control system to automatically coordinate electrical stimulation with hydraulic exoskeleton using a mobile computing platform.**

The aim of this task is to untether HNP1 and design and implement mobile computing platform for HNP2 system to be utilized outside the laboratory.

Supporting hardware and software was developed for control and data acquisition for evaluation of the HNP1 (**Figure 18**) as described in the Final Report Award Number: W81XWH-05-1-0389. Custom circuitry was developed and integrated with instrumentation and computers at the Motion Study Laboratory at the Louis Stokes Cleveland VA Medical Center. This allowed for the xPC Target (The MathWorks, Inc., Natick MA, USA) prototyping environment to execute Simulink models in real time for controlling the HNP1 system. The target PC was used for sensor signal acquisition and the output of control states to the exoskeleton while the xoskeleton was tethered to the target PC. All communication between the target PC and exoskeleton was through a multi conductor cable at a frequency of 200 Hz during laboratory experiments. The host PC runs Matlab®/Simulink® and was responsible for building the target application into the target PC and controlling the target application during operation. The host and target computers communicated via the TCP/IP protocol. The host PC ran a graphical user interface (GUI) which was developed to simplify the building, calibration, implementation, and testing of the HNP1 controller. The GUI sent commands to and acquired signals from the target PC during real-time implementation. A wearable muscle stimulation unit delivered FNS to the targeted paralyzed muscles to drive limb motion. The activity states were selected by the user through button polling and displayed on a liquid crystal display. Steps were triggered either by a push button, automatically cycled until stopped or initiated by a sensor. When the STOP button was pressed during walking, the stimulation pattern transitioned into the standing mode at the end of the step. A scroll button was programmed to provide subject options to walk, climb stairs or sit down.

The HNP1 controller consisted of three subsystems that communicated with each other to coordinate motion: a finite state knee controller (FSKC) for the dual state knee mechanism, a finite state postural controller (FSPC) for the variable constraint hip mechanism, and the FNS controller.

New Untethered Hardware

An Arduino-based embedded control system was designed for HNP2 to achieve untethered operation outside of the laboratory as shown in **Figure 19**. The embedded controller board communicates with a PC only for controller development and downloading and is designed to be compatible with mobile devices such as smartphones which will serve as the user interface. The stimulus generating circuitry currently employed in our wearable muscle stimulator (UECU) will be integrated into the untethered system.

The main control unit is the ATmega2560 processor. This is a high-performance, low-power Atmel 8-bit AVR RISC-based microcontroller which combines 256KB ISP flash memory, 8KB SRAM, 4KB EEPROM, 86 general purpose I/O lines, 32 general purpose working registers, real time counter, six flexible timer/counters with compare modes, PWM, 4 USARTs, byte oriented 2-wire serial interface, 16-channel 10-bit A/D converter, and a JTAG interface for on-chip debugging. It supports 16 channels of pulse width modulated (PWM) digital output for hydraulic valve or motor control. The device achieves a throughput of 16 MIPS at 16 MHz and operates between 4.5-5.5 volts.

An ATmega328 microcontroller is used as a co-processor for data fusion and filtering, and communicates with the main processor by UART port. The MPU-9150 9-axis inertial measurement unit (IMU) includes accelerometer, gyroscope and compass to provide capabilities to measure 3D linear accelerations, angular velocities and orientations of the corset-mounted system to simulate dynamics of movement of

Figure 20. Embedded controller boards.

Figure 19. Block diagram of mobile computing platform for HNP2.

the body center of mass.

Embedded controller boards (**Figure 20**) were designed, constructed and tested over the past year. The control unit communicates with universal external control unit (UECU) stimulation boards through Universal Asynchronous Receiver/Transmitter ports (UART). There are two kinds of stimulation boards that can provide stimulation with either percutaneous or surface electrodes. In addition, there is an implant communication board that can send command signals to an implanted receiver stimulator. All stimulation boards can be used by themselves or in combination with others.

The signal conditioning board will generate all required valve control and drive signals, sensor signal processing, communication between embedded controller and stimulation board, and power conditioning for all circuitry, sensors and valving. In addition, the signal conditioning board will include wireless sensor board subsystem to provide communication with wireless finger switch and wireless accelerometers and gyroscopes that can be mounted on the exoskeleton for feedback control.

New Untethered Software

Significant progress was made in software development and testing.

- Firmware was developed for Embedded Controller Board main processor and IMU subsystem coprocessor.
- A Matlab® interface was developed for compiling and downloading Simulink code to microcontroller.
- Software filters were developed and tested for analog signals
- A Kalman filter was developed for the 9-axis IMU
- Matlab® software for data collection and plotting via Bluetooth was created
- Version 1.0 of the embedded wireless data logging program, which included sampling, filtering, transmitting, and processing of force sensing resistors (FSRs), IMU, and potentiometer signals, was developed and tested.
- Version 2.0 of the embedded wireless data logging program was developed which can acquire 14 analog channels plus IMU data with Kalman filtering at 100Hz.
- We initiated investigation for real-time on-board gait event detection.

Hardware and Software Testing

An able bodied individual wore a brace instrumented with embedded controller board, FSRs, IMU and potentiometers at knee and hip joints to simulate paraplegic gait for real-time-on-board gait event detection (**Figure 21**). For comparison, reflective markers were attached to the brace and the subject's feet for VICON motion analysis in the Motion Study Laboratory of the LSCVAMC.

Figure 21. Subject walking with instrumented brace with embedded controller collecting and transmitting data to PC.

Real time gait detection was run on the embedded controller with sensor sampling rate and Bluetooth transmission at 100Hz. Heel strike could be easily detected with FSRs and IMU provided reliable orientation of the trunk (**Figure 22**).

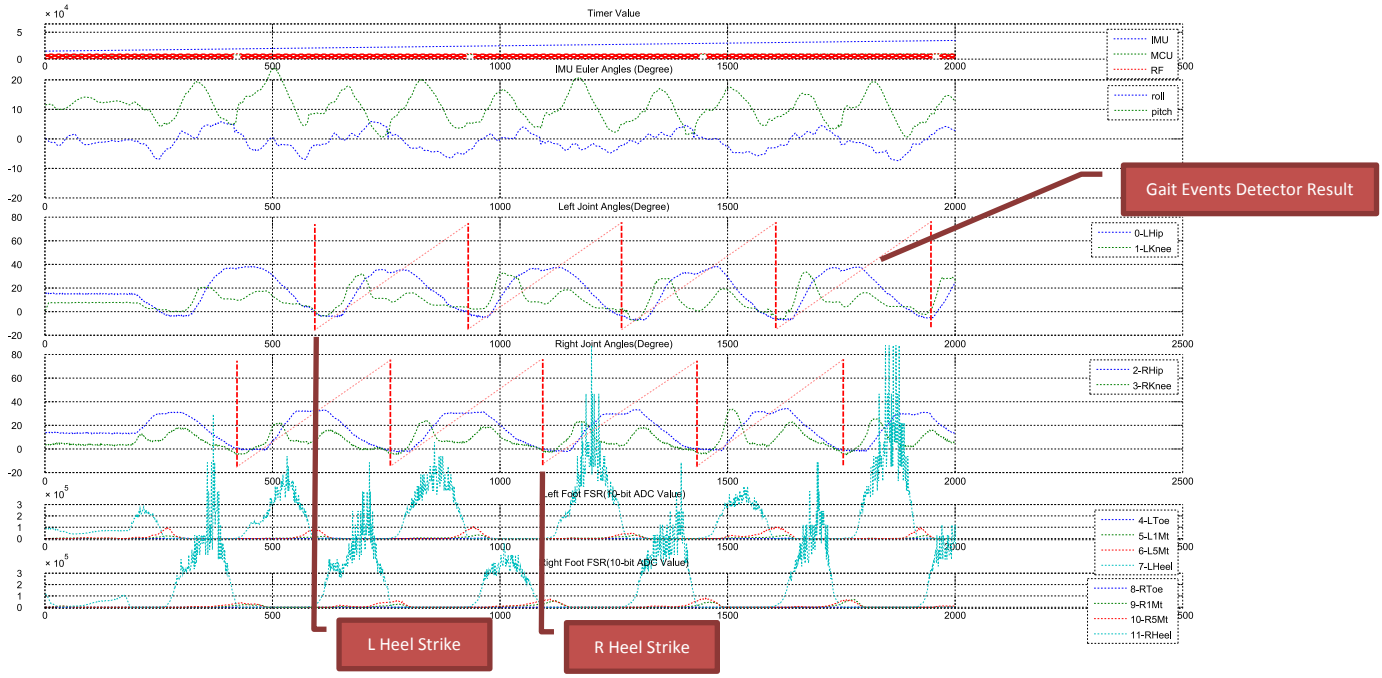

Figure 22. Data collected with untethered embedded controller during slow walking.

KEY RESEARCH ACCOMPLISHMENTS:

- Hydraulic hip-knee coupling mechanism has been designed, prototyped, tested and characterized
- Hip and knee moments for HNP2 were specified for walking and stair climbing and an algorithm was developed to optimize cylinder mounting for a 3 bar linkage transmission at the hip and knee to meet torque vs angle requirements.
- Custom rotary actuators and proportional valves were designed, constructed and tested for consideration as replacement for off-the-shelf hydraulic components.
- Off-the-shelf high speed valves were tested with pulse width modulated opening and closing for ability to provide proportional damping at the knee.
- Structural components of the exoskeleton including corset and uprights were designed for ease of manufacture and construction, fitting and donning.
- Arduino based hardware was designed, constructed, and tested for mobile computing platform.
- Software for mobile computing platform was written for data collection and analysis to be used for control of HNP2.

REPORTABLE OUTCOMES:

- **Manuscripts, abstracts, presentations;**

Poster presentations:

"A Hybrid Neuroprosthesis for Gait Restoration after Spinal Cord Injury"
April 13 2013

Research ShowCASE
Case Western Reserve University, Cleveland, OH

"Coordinating the hip and knee joints during gait using a hybrid neuroprosthesis"
April 16, 2014
Musculoskeletal Research Day (Department of Orthopaedics)
Case Western Reserve University, Cleveland, OH

"Coordinating the hip and knee joints during gait using a hybrid neuroprosthesis"
April 18, 2014
Research ShowCASE
Case Western Reserve University, Cleveland, OH

"Coordinating the hip and knee joints during gait using a hybrid neuroprosthesis"
May 22, 2014
VA Research Week
LSCDVAMC, Cleveland, OH

"Coordinating Hip and Knee Joints with a Hybrid Neuroprosthesis" (submitted)
August 26-30, 2014
IEEE EMBC
Chicago, IL

- **licenses applied for and/or issued;**
  - Utility patent application "Power Assisted Orthosis with Hip-knee Synergy"

- **degrees obtained that are supported by this award;**
  - ***Opportunity for students to get involved in research***
    - Sarah Chang, B.S., graduate student, PhD., candidate in Biomedical Engineering
    - Mark Nandor, M.S., graduate student Ph.D., candidate in Mechanical Engineering
    - Lu Li, B.S., graduate student, M.S. candidate in Mechanical Engineering
    - Kiley Armstrong, undergraduate Mechanical and Biomedical Engineering student
    - Maria Lesieutre, undergraduate student majoring in Mechanical with minor in Biomedical Engineering.
    - Alexander Spalding, B.S., Mechanical Engineer

- **funding applied for based on work supported by this award;**
  - Maria Lesieutre, applied and received SOURCE funding from CWRU to do summer research project on control of knee stiffness and damping for the stand-to-sit maneuver with HNP.
  - Sarah Chang, applied and received a pre-doctoral fellowship from a Training Program in Musculoskeletal Research from the NIH (5T32-AR007505-28) pursue her graduate studies.

- **employment or research opportunities applied for and/or received based on experience/training supported by this award**
  - Alexander Spalding, B.S.

CONCLUSION:

Considerable effort has been expended and significant progress has been made in all three tasks.

Specifically, the hip-knee coupling mechanism was designed, evaluated and characterized. The coupling ratios, passive resistance and delay between hip and knee movements varied somewhat with angular velocity, but were within specifications. Further effort is underway to characterize the source of resistance and delay and to minimize them.

A number of custom hydraulic components including rotary actuators and proportional valves were designed, constructed, tested and characterized for inclusion in the hydraulic circuit in an effort to reduce size and weight. These devices did not meet the specifications for the HNP2 and further development of these components is beyond the scope of this study and have been deferred. Off-the-shelf components will be substituted instead. The structural components of the HNP2 were designed and are ready to be fabricated. These will provide ease of fitting and doffing/donning.

A mobile computing platform based on Arduino hardware was designed and fabricated to interface with existing stimulation control hardware. Software for sensor data collection was written and tested using sensors mounted on HNP1 during able bodied walking.

REFERENCES:

1. Kobetic R, To CS, Schnellenberger JR, Audu ML, Bulea TC, Gaudio R, Pinault G, Tashman S, Triolo RJ (2009). Development of hybrid orthosis for standing, walking, and stair climbing after spinal cord injury. *Jour Rehab Res and Dev* 46(3):447-462. DOI:10.1682/JRRD.2008.07.0087.
2. To CS, Kobetic R, Bulea TC, Audu ML, Schnellenberger JR, Pinault G, Triolo RJ (2011). Stance control knee mechanism for lower-limb support in hybrid neuroprosthesis. *Journal of Rehabilitation Research & Development*, 48(7):839-850. DOI:10.1682/JRRD.2010.07.0135.
3. To CS, Kobetic R, Bulea TC, Audu ML, Schnellenberger JR, Pinault G, Triolo RJ (2012). Sensor-based stance control with orthosis and functional neuromuscular stimulation for walking after spinal cord injury. *J of Prosthetics and Orthotics*, 24(3):124-132.
4. To CS, Kobetic R, Schnellenberger J, Audu M, Triolo RJ. Design of a variable constraint hip mechanism for a hybrid neuroprosthesis to restore gait after spinal cord injury. *IEEE/ASME Transactions on Mechatronics*, 13(2):197-205, 2008.
5. To CS, Kobetic R, Bulea TC, Audu ML, Schnellenberger JR, Pinault G, Triolo RJ (2014). Sensor-based hip control with hybrid neuroprosthesis for walking in paraplegia. J Rehabil Res Dev. 51(2)229-44. http://dx.doi.org/10.1682/JRRD.2012.10.0190.
6. Bulea TC, Kobetic R, To CS, Audu M, Schnellenberger J, Triolo RJ (2012). A variable impedance knee mechanism for controlled stance flexion during pathological gait. *IEEE/ASME Transactions on Mechatronics*, 17(5):822-832. DOI:10.1109/TMECH.2011.2131148.
7. Bulea TC, Kobetic R, Audu ML, Triolo RJ. Stance controlled knee flexion improves stimulation driven walking after spinal cord injury. Journal of NeuroEngineering and Rehabilitation, 10:68, 2013.

8. Bulea TC, Kobetic R, Audu ML, Schnellenberger JR, Triolo RJ (2013). Finite state control of a variable impedance hybrid neuroprosthesis for locomotion after paralysis. *IEEE Trans Neural Syst Rehabil Eng*. 21(1):141-51. doi: 10.1109/TNSRE.2012.2227124. Epub 2012 Nov 15. PubMed PMID: 23193320.
9. Winter DA. T*he Biomechanics and Motor Control of Human Gait: Normal, Elderly and Pathological*, 2nd ed. Waterloo: University of Waterloo Press, 1991.
10. Kobetic R, Marsolais EB (1994). Synthesis of paraplegic gait with multichannel functional neuromuscular stimulation. *IEEE Trans Rehab Eng.* 3(2): 66-79.

APPENDICES: Appendix A – Three Bar Linkage Optimization for Joint Transmission

Introduction

In the first prototype, the HNP1, we utilized a 3 bar linkage to translate the linear force of the hydraulic cylinder to a torque around the knee joint, and a rack and pinion gear set to accomplish the same job at the hip joint. Each transmission has its advantages and disadvantages. The 3 bar linkage arrangement at the knee joint weighs less than a rack and pinion gear set, but the specific implementation used in the HNP1 contains a singularity of zero moment arm (and hence zero torque resisting capability) at 72° of knee flexion. While the hip implementation of a rack and pinion gear set has no singularity and has a constant moment arm profile regardless of joint position. it is heavier and contains more mechanical backlash compared to the 3 bar transmission.

It was hypothesized that a 3 bar transmission can be designed that has the weight and backlash advantages over a rack and pinion gear set, but eliminates the singularity found in the HNP1 design. To accomplish this, software tools were designed to select and optimize joint arrangements.

Knee Joint

Definition - The rotational center of the knee joint is considered the origin of the knee coordinate system. The femoral upright is considered the positive Y-axis extending upward, with positive X extending anteriorly to the knee joint. The femoral upright is considered fixed in space at all times during selection and optimization of the knee joint. The shank upright is considered to be rotating around the origin. Full extension of the knee is when shank upright is collinear with the femoral upright and both are vertical. Hyperextension of the knee is considered to be positive (counter clockwise) rotation from full extension, and knee flexion is considered negative (clockwise) rotation.

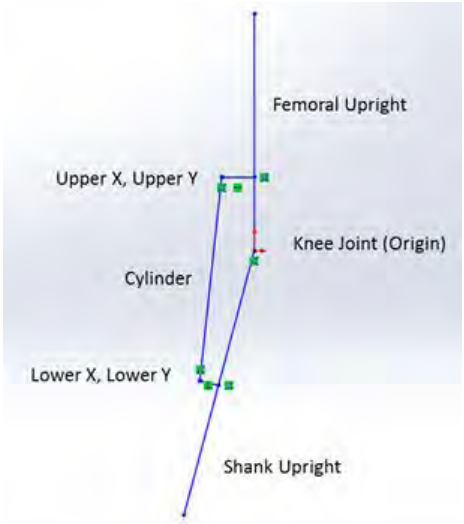

Figure A1. 3D linkage definitions.

The cylinder pickup points are defined by the (x, y) pairs as shown in the diagram. On the femoral upright, the cylinder is located and the (x, y) pair (Upper X, Upper Y). Because the femoral upright is considered fixed in space, Upper X and Upper Y are considered fixed as well – they are initially defined and treated as constant throughout the range knee motion. Coordinates (Lower X, Lower Y) define the location of the cylinder pickup point on the shank upright. These coordinates are initially defined with knee at neutral and determined as a function of knee angle between 10° of hyperextension to 110° of flexion. Defining the cylinder size and maximum pressure rating, torque vs angle relationships can be constructed for various mounting configurations.

Linkage selection - The linkage profile selection algorithm consists of sweeping the (Upper X, Upper Y) and (Lower X, Lower Y) pairs through a predetermined pattern of values and determining the moment arm profile for each set of points. First the linkage must satisfy maximum and minimum length criteria of

the cylinder. Next, the sets that produce a singularity in the associated torque profile are discarded. The best torque vs angle profiles are defined as those with highest average torque that meets the specified torque requirements or has the least squares error of the calculated torques and the specified torques. If the calculated torque is greater than the required torque at a point, then the error is considered to be zero. Only when the calculated torque is less than the required torque, it contributes to the overall error.

Similarly, the algorithm was adapted for design of the hip cylinder linkage by adjusting the joint range of motion and torque requirements.

Knee linkage optimization

The optimization parameters were as follows:

1) Range of motion is 10° hyperextension to 110° of flexion.
2) Torque vs angle required is defined in Figure 10.
3) Cylinder with 0.875" bore rated at 1000psi from Clippard.
4) (Upper X, Upper Y) location – for size requirements, the X coordinate is limited from -3 to +3 inches, and the Y coordinate ranges from -6 to +3 inches.
5) (Lower X, Lower Y) location – for size requirements, the X coordinate is limited from -3 to +3 inches and the Y coordinate is limited to +6 to +12 inches.

A search with a 0.875" bore cylinder with 3" stroke with the lowest modified least squares error yielded attachment points (Upper X, Upper Y) = (-.9, 1.45) and (Lower X, Lower Y) = (-1.612, -9.592) with the torque vs angle profile shown in **Figure A2**a with linear relationship of cylinder length vs knee angle shown in **Figure A2b**.

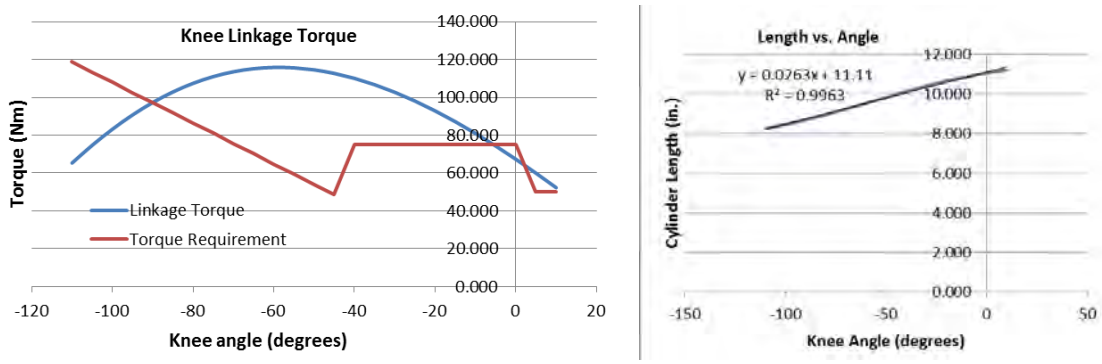

b)

Figure A2. Torque **a)** and cylinder length **b)** as a function of knee angle for a 0.875" bore, 3" stroke cylinder from Clippard.

Hip linkage optimization

The optimization parameters were as follows:

1) Range of motion is 20° of extension to 100° of flexion
2) Torque vs angle is defined in Figure 11.
3) Cylinder requirement is driven by the hip-knee coupling (HKC) requirements. This example will search For a 1:1 HKC a 0.875" bore, 3" stroke cylinder from Clippard was selected.
4) (Upper X, Upper Y) location – for size requirements, the X coordinate is limited from -2 to +3 inches. The Y coordinate is limited to -2 to 2 inches.
5) (LowerX, LowerY) location – for size requirements the X coordinate is limited from -2 to 3 inches and the Y coordinate is limited form +4 to +12 inches.
6) Because the knee cylinder length is monotonically decreasing from max extension to max flexion, the hip cylinder must be decreasing as well to satisfy the equal fluid volume constraint during coupling.

As it turns out, the driving requirement here is satisfying the coupling requirement – the use of such a large cylinder makes it easy to satisfy the torque requirements. As such, the chosen linkage was selected because it satisfied all of the above requirements, and packaged the best into the brace design – it didn't cross the center line of the linkage, there were no spacing concerns at either pick up point, etc. The linkage using the coordinates (Upper X, Upper Y) = (-1.15, -1.2) and (Lower X, Lower Y) = (-1.712, -9.685) resulted in torque profile shown in **Figure A3a** which exceeds requirements at all angles of the hip. The cylinder length change with hip angle is highly lines as shown in **Figure A3b**.

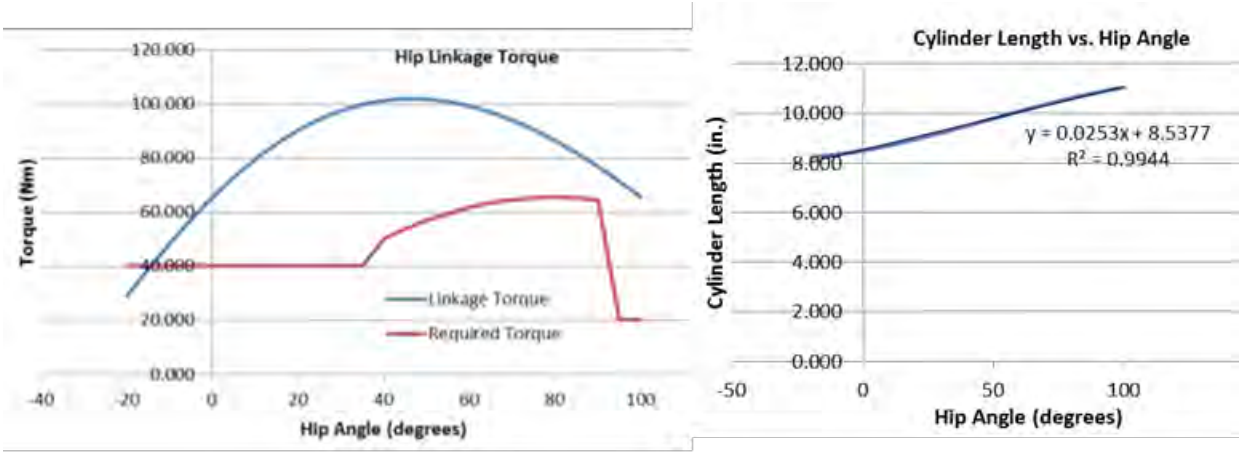

a) **b)**

Figure A3. Torque **a)** and cylinder length **b)** as a function of hip angle for a 0.875" bore, 3" stroke cylinder from Clippard.

Conclusion

The knee and hip linkages presented in this Appendix meet the specified torque requirements at the hip and knee with the cylinder movement that is highly linear within the range of joints motions and satisfy requirements for the 1:1 hip-knee coupling ratio.

Appendix B – Rotary Actuator Design and Evaluation

Introduction

The most appropriately sized commercial model of actuator that meets specification for use in the HNP2 would be from Micromatic a MPJ-22, capable of 168 Nm of output torque at 1000 psi. This unit weighs 1.45 kg, and has a 76 mm outer diameter, and a 67.8 mm overall length. While the size and weight are a bit large, most worrying about the performance of the actuator is the stated leakage. At 1000 psi, the actuator has a manufacturer specified leakage of
148 cc/min. With a total internal fluid displacement of 9.13 cc, this implies that under maximum pressure, the entire unit could discharge due to leakage in under 3.7 seconds. In the HNP2 application (using this actuator as a knee joint), this would be unacceptable, leading to the collapse of the user.

Design specifications

The maximum torque of 120 Nm was specified for knee from **Figure 10**. The maximum pressure was limited to 1500psi by Buna-N O-ring based seal design. In addition, the passive resistance of the device should be on par with or better than linear hydraulic linkages of HNP1 to minimize effort of stimulated muscles to overcome friction.

A vane rotary actuator was adapted for this design with the net torque on the vane

$$\tau_{net} = \tau_r - \tau_l = \frac{1}{8} tp(d_o^2 - d_i^2)$$

The prototype actuator is designed to have the dimensions shown in **Table B1**. The ID of 1.25 in. was the smallest diameter that could be used while still retaining enough space to insert a shaft seal. The thickness of 0.78 in was chosen to give the overall actuator a width of 2.5 in, targeted as the maximum allowable for the exoskeleton. With those two constraints selected, and the torque criteria, the OD was not a free parameter and determined by solving the torque equation.

Table B1. Design parameters

Parameters	Dimension
Outer Diameter (d_o)	2.98 inches
Inner Diameter (d_i)	1.25 inches
Thickness (t)	0.78 inches
Pressure (p)	1500 psi
Designed output Torque	126 Nm

Rotary Actuator Manufacturing

The SolidWorks drawing in **Figure B1** illustrate the conceptual prototype rotary actuator. It consists primarily of 3 pieces – a middle section that contains the vane, and two mirror image end pieces that are held in place with 3 #8 bolts. The vane contains a machined hex to transmit torque to the drive axles, which consist of two identical pieces that stick out of the end faces. The vane contains machined grooves, into which seals are inserted. These machined grooves are on all faces, allowing for complete coverage of all sides. Internal channels were drilled into the middle body, which connect the internal

chambers to the external hydraulic circuit. The body is tapped to accept standard SAE#6 straight thread hydraulic fittings. To maintain alignment and concentricity between all 3 pieces, guide pins pressed into the outer faces locate themselves into reamed holes placed on the body. To seal the body and the outer faces, channels are cut into the outer faces, designed to accept laser cut rubber that act as static seals.

All pieces were manufactured on a 3 axis CNC mill out of 6061 aluminum. To maintain tight tolerances, all inside features were machined in a single setup out of oversized stock. All indexes were machined in, leaving no error in the setup. All pieces were faced at the end of every job, ensuring flat and parallel mating surfaces. All tolerances are within .001" of nominal.

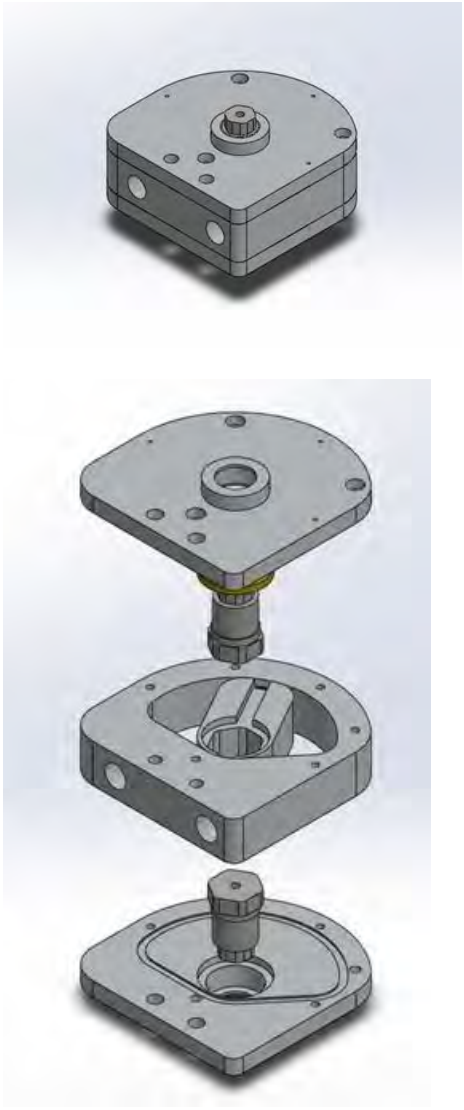

Figure B1- Assembled and Exploded views of the prototype actuator.

The seals used during testing consist of Buna – N rubber laser cut to fit the outside static seal faces and the vane dynamic seal faces. Parameters such as seal shape and amount of interference were kept as experimental variables to determine testing results. Some configurations used a liquid silicone sealant (Loctite Red or Blue) in an effort to enhance sealing performance, with varying results.

Rotary Actuator Bench Test

The prototype actuator was evaluated initially for locking pressure, and later for passive resistance. Passive resistance testing was only performed on the configuration that had the best locking pressure performance, under the assumption that any configuration that did not meet locking pressure criteria would not be of any use.

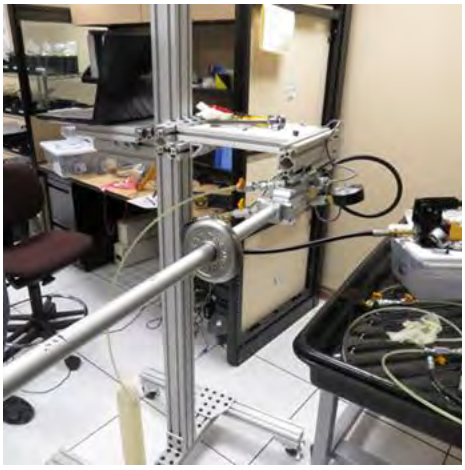

Figure B2. Experimental setup to test locking torque.

The test setup is shown in **Figure B2**. An aluminum arm was fabricated to attach to the axle of the actuator, providing a measurable moment arm for testing. Hydraulically, the chambers were simply connected to each other via hose, with a manually operated valve in between. The valve only altered flow in one direction, with a check valve allowing free flow in the other. An analog pressure gauge allowed for easy measurement without an attached computer, while

digital pressure gauges were attached to both chambers, allowing for pressure differential to be measured. Quick disconnect ports on both chambers allowed for easy priming and draining.

This test setup allowed for quick and easy testing of multiple seal configurations. Two different vanes were cut, with the seal grooves allowing for different levels of seal interference. The rubber used was nominally 0.125 inches thick for the top and bottom pieces, and 0.0625 inches thick for the side pieces. Originally the seals were cut to nominal dimensions of the grooves, but post examination of the seals showed that the laser cutter used to cut the pieces to smaller than nominal sizes. Calibration and measurement of several test pieces led to the second iteration of seal design, in which the design sent to the laser was slightly larger than nominal, leaving a nominal sized seal after cutting. The third seal was created to be undersized, using Poisson's ratio for rubber to estimate the XY expansion of the rubber due to Z axis compression. In addition to the vane and seal variables, a liquid silicone sealant was applied as well. Initially, Permatex 81160 High-Temperature Red RTV silicone gasket was tried. However, examination after testing exposed that this silicone had a corrosive effect on the rubber. A call to the company revealed two causes of this – first, that the Red RTV is not chemically compatible with the Buna-N rubber in the seal, and secondly that RTV only has a usable shelf life of 6 months after opening. While there is no documentation to support this, it is highly likely that the tube of silicone used was over the expiration date. Permatex customer support recommended Blue RTV for our use, and a brand new tube was acquired for testing.

Once the best seal configuration was determined from static testing, that configuration was placed on the Biodex dynamometer to collect passive resistance data as shown in **Figure B3**. The Biodex was run in a constant speed mode, rotating the actuator through its full range of motion, while collecting angle, angular velocity, and torque data. Speeds of 30, 60, 90, 120, 150, and 180 degrees per second were tested. At each speed, the actuator was put through at least 12 complete flexion/extension cycles. The same hydraulic circuit was also used in this test setup, with the two sides of the actuator connected by a single hydraulic line, with the same manually operated valve located in between. For this testing, the valve was simply opened fully. A calibration run with no actuator attached to the Biodex conducted at 30°/s allowed for the weight of the Biodex arm to be calculated and subtracted out from the measured torque, leaving the passive resistance of the actuator.

Figure B3. Rotary actuator attached to Biodex dynamometer.

Results of Bench Tests

The following vane and seal configuration were tested:

Vane Configurations	
Vane 1	Designed for .01" seal interference
Vane 2	Designed for .02" seal interference

Seal Configurations	
Seal 1	Cut exactly to dimensions of pockets
Seal 2	Oversized to account for XY tolerance of Laser Cutter
Seal 3	Undersized, using Poisson's ratio to account for seal expansion

Results of the bench testing are shown **Table B2**. Vane 1 (.01" seal interference), Seal 2 (oversized), and RTV Blue produced the best results in static testing.

Table B2. Results of bench testing

Testing Date	Vane	Seal	Epoxy	Result
3/6/14	Vane 1	Seal 1	RTV Red	Sealant ate away at rubber, further examination shows RTV Red not compatible with Buna N seal
3/20/14	Vane 1	Seal 1	RTV Blue	Seals held up to 200 psi dynamically
3/25/14	Vane 1	Seal 2	RTV Blue	Seals held up to 350 psi dynamically
3/28/14	Vane 2	Seal 2	RTV Blue	Very high passive resistance, post examination showed seal destroyed by frictional forces
4/1/14	Vane 2	Seal 3	None	No holding capability, statically or dynamically
4/7/14	Vane 2	Seal 3	RTV Blue	Same result as 4/1/14, no pressure holding

Static testing of the best vane/seal/epoxy combo was performed by hanging weights on the horizontal moment arm provided by the rotary actuator while pressure was measured with digital pressure transducers mounted on both chambers of the rotary actuator. The rotary actuator was able to resist 5ft-lbs at 20psi before the moment arm began to move due to internal leakage.

Table B3. Mean (± 1 S.D.) passive resistance

Angular velocity (°/s)	Passive resistance to extension (Nm)	Passive resistance to flexion (Nm)
30	7.2 (2.6)	12.5 (3.2)
60	6.8 (2.0)	12.3 (2.3)
90	6.8 (1.7)	12.6 (2.1)
120	7.0 (1.6)	13.0 (1.6)
150	7.3 (1.7)	13.9 (2.3)

Dynamic testing using the Biodex dynamometer measured resistive moment to counterclockwise (considered joint extension) rotation, and clockwise (considered flexion) rotation at five different angular velocities. Mean (± 1 S.D.) passive resistance is shown in **Table B3**. The data showed little variability in passive resistance with angle and angular velocity. However, passive resistance to clockwise rotation (+) was about twice that in counterclockwise (-) direction as shown in **Figure B4** for angular velocity of 60°/s.

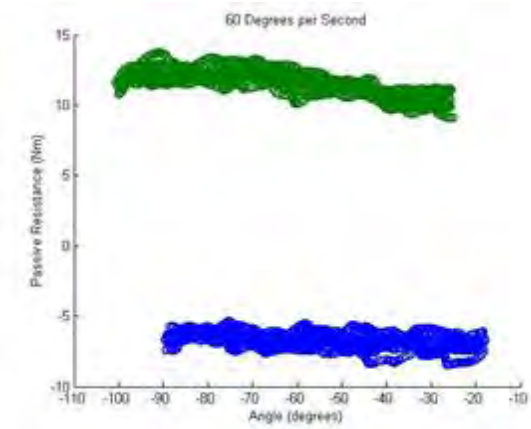

Figure B4. Passive resistance vs. angle at angular velocity of 60°/s.

Discussion of rotary actuator

The prototype rotary actuator failed to meet the necessary specifications, thus it will not be considered for use in the HNP2. It is only able to statically seal up to 20 psi, and passive resistance numbers are significantly larger than previous hydraulic linkages.

All data indicates that the issue lies within the dynamic seal on the vane. Visual inspection show that throughout testing, the static seals around the edge of the device held up quite well and prevented fluid from leaking from the middle chambers out the edge of the side pieces. Leakage out the axle ports was present but subjectively did not appear any worse than what is seen out of the rod port of currently used brass linear cylinders.

Appendix C – High Speed Proportional Valve Testing and Evaluation

Introduction

The objective of this effort was to create a hydraulic circuit that can effectively restrict and control the velocity of an extending/contracting hydraulic cylinder for damping. Commercial valves that can vary orifice size to achieve this control do exist; however a valve that provides sufficient resolution in the flow range needed for HNP2 (0.3-0.7 GPM) has not been located. An alternative to a variable orifice valve is a fast acting 2 way/2 position valve. It is hypothesized that a fast acting valve can effectively control cylinder pressure/speed while switching fast enough such that fluctuations are not noticeable and the motion is smooth.

Methods

To test this hypothesis, a 3 way/2 position, normally closed valve was acquired from Clean Air Power, in California (cleanairpower.com), along with a mounting block. According to the specifications, the valve is capable of opening in 3 milliseconds and closing in 2 milliseconds – theoretically allowing for a maximum operating frequency of 200 Hz. While ideally a 2 way/2 position NC valve would be selected, the company does not offer that configuration. In this 3 way configuration, the vent port was closed off, allowing it to act as a 2 way/2 position NC valve. The valve was controlled by a pulse width modulated (PWM) signal, varying the duty cycle of a square wave to control the on time of the valve.

Figure C1. Set-up for high speed valve test.

To test the valve, a hydraulic circuit was constructed that shuttled fluid between a small 9/16” bore cylinder and a larger 7/8” bore cylinder. The 9/16” bore cylinder served as the cylinder to be controlled, while the large one simply served as an accumulator for fluid storage. Both cylinders were utilized in a single acting manner, with the blind side of each simply vented to atmosphere. In between the cylinders was the valve, connected by hoses to the rod side of each. The test cylinder (9/16”) was loaded with weight such that when the valve opened, the rod extended downward as shown in **Figure C1**.

To control the valve, a PWM signal of varying frequency and duty cycle was produced by a function generator (**Figure C2**). That signal was fed into a MOSFET which performed the high power switching for valve opening and closing. A reflective marker was attached to the rod of the cylinder to track its motion with the VICON Motion Analysis System. In addition, pressure transducer was attached at the cylinder port to monitor pressure collected by VICON. A simple digital on/off signal indicating valve state was also generated and recorded.

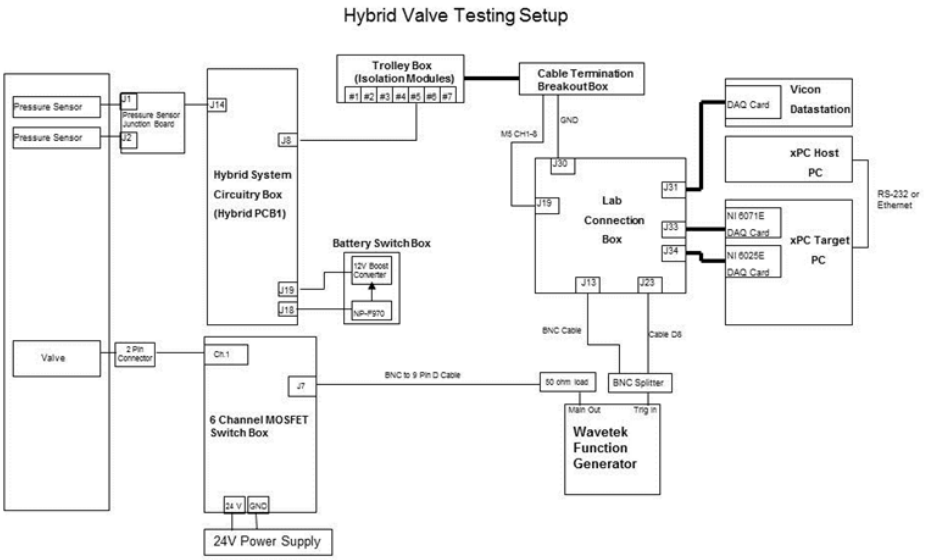

FigureC. Schematic of high speed valve test set up.

Tests were performed at frequencies of 10, 25, 50, 75, and 100 Hz. At each frequency, duty cycles of 10, 25, 50, and 75% were tested. For each test, the cylinder was fully retracted and allowed to fully extend. A control run of fully open (100%) was also performed.

Results

The cylinder rod movement at 10 Hz at different duty cycles is shown in **Figure C3**.

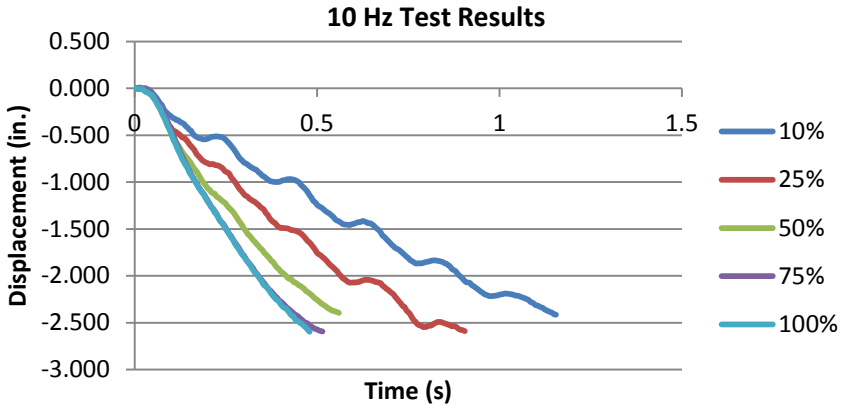

Figure C3. Cylinder displacement at 10Hz at different duty cycles.

The cylinder is extending at a slow rate at 10% duty cycle, and speeding up as the duty cycle increases. However, there is no difference in movement at 75% and 100% (full open).

At 25 Hz as shown in **Figure C4**, there is very little variation in the displacement curves with duty cycle.

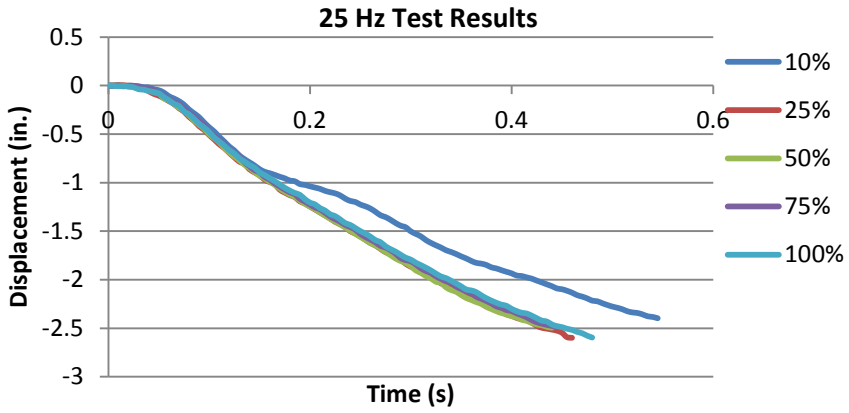

Figure C4. Cylinder displacement at 25Hz at different duty cycles.

Similarly at 50 Hz as shown in **Figure B5**, there is no change in cylinder displacement by changing duty cycles.

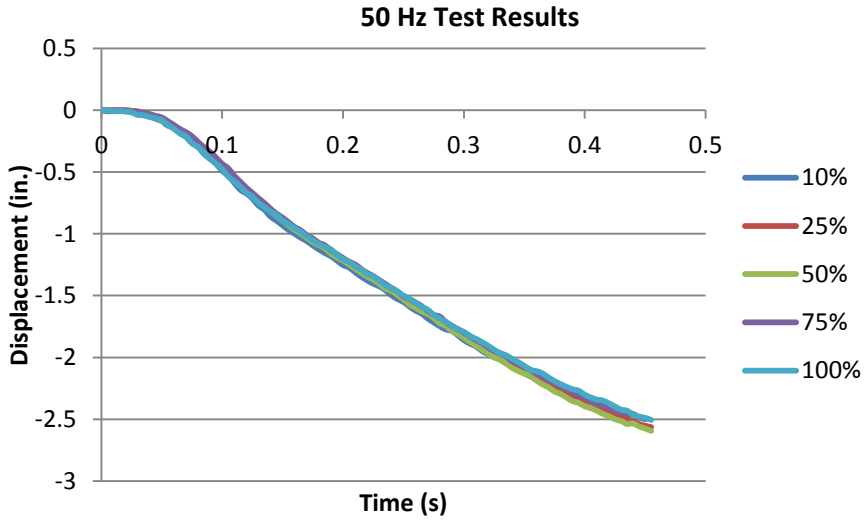

Figure C5. Cylinder displacement at 50Hz at different duty cycles.

At 50 Hz, it is clear the valve is not attenuating the cylinder extension speed at all and acts as fully open. It's clear that at 50Hz and higher, the valve is simply opening once and unable to close again before the next open signal arrives, thus, lacking the needed response time.

Discussion

These results are unexpected – the specifications of the valve claim it can open and close in 5 ms, yet at 50 Hz (20 ms period) the valve is unable to close. Consulting with an engineer at Clean Air Power, we learned that in its typical application, this valve is used for shift bands/clutches in automatic

transmissions. As such, it is used in situations where there is always a high pressure supply behind it to return the valve to its normally closed state. In our damper application, the high pressure supply was not present.

Conclusion

The valve is not designed to work in the configuration proposed for knee damping application for HNP2. Specifically, it is clear from the test results that not having the necessary high pressure supply to return the valve to its closed position resulted in very (unacceptably) slow valve close times. As a damper, it could only operate at low operating frequencies (10 Hz), where the test results show that the valve has enough time to close, but at that frequency, the output motion is unacceptable jittery.

Appendix D – Prototype Proportional Valve Design and Evaluation

Introduction

In the HNP1 a MR damper was incorporated in the exoskeleton as part of the variable impedance knee mechanism (VIKM) to provide a proportional torque response. There were clear advantages of this mechanism over the simple on/off hydraulic locking mechanism in loading response and pre swing phases of gait (Bulea 2013) and during stair descent (Bulea 2014). The main disadvantage of the MR based mechanism was that it required a significant power to keep the knee locked during standing. Thus, an attempt was made to replicate the ability of the VIKM and its damper, but using traditional hydraulic fluid. Instead of modulating the viscosity of the fluid, the area of the orifice the fluid is traveling through would be modulated by means of a proportional valve.

We have not been able to identify a commercially available proportional valve that meets requirements of flow rate, size, weight and pressure rating to perform damping at the knee. In particular, the flow rate (0.3- 0.7 gpm) we are interested in controlling is much smaller than what is typically available in industrial hydraulics (2-50 gmp). On the other hand, some of the smaller pneumatic/hydraulic valves do not meet the required pressure rating for knee damping application. To meet specifications of low flow, high pressure, small size and weight capability, a custom prototype proportional valve was designed, built and tested.

Methods

Valve design – The model of the valve is shown in **Figure D1**. The design consists of aluminum housing, drilled to allow fluid to pass through from one side to another. Inside the circular chamber is a printed spool, manufactured using advanced stereolithography (SLA) additive machine, with a rigid core and a soft rubber outer layer to seal against the walls of the chamber. The spool has a swept cut that modulates the cross sectional area of the intended flow path. In initial prototypes, cross sectional area was designed to be linear with angular rotation of the spool.

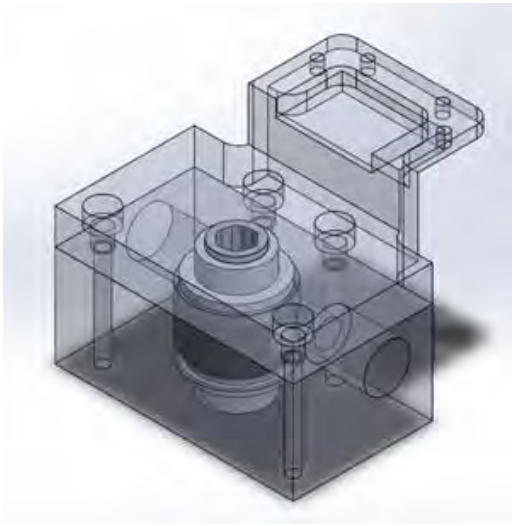

Figure D1. CAD model of proportional valve

Instead of a solenoid providing the motion of the spool, motion is provided by a servomotor. This selection was made to provide a greater degree of control and decrease the power consumption of the device. The selected digital servo (Dynamixel AX-18) communicates via serial port and is capable of operating in closed loop position control and providing feedback on instantaneous position, speed, and torque.

Valve test setup - To evaluate this valve, an AC hydraulic power unit capable of providing constant pressure output up to 1500 psi and flow rate up to 1 gpm was used to define pressure vs. flow properties of the valve. Digital pressure sensors on either side of the valve were used to measure

pressure. Additionally, a flow sensor (Omega Engineering) was used to measure the flow through the valve. Setting the pressure on the valve, and adjusting the position of the spool should result in modulated flow through the valve.

Results

In the first batch of spools there were manufacturing problems with X-Y tolerances in the order of 0.01" - 0.02" in extra material – meaning outer diameters were all too big, and inner diameters too small. . To circumvent this problem, the second round of spools were designed to be placed in a jig and machined after printing. This ensured a tight fit between the spool and the cavity. The cavity had a diameter of .75", and spools were constructed with outer diameters of .74", .745", .75", .755", .76", and .765". The spools with .74", .745", and .75" outer diameters did not modulate the flow at all, whereas the .755" and .76" diameters would not move due to the amount of friction. The results of the .755" spool are shown in **Figure D2**. A spool position of 0 degrees is considered fully shut. As shown, the spool does have a small effect in modulating the flow at a constant pressure difference of 200 psi, but the range is small, less than 30° of motion before the flow is maxed out at 1 gpm. In the fully closed position, the valve is allowing over 0.86 gpm of flow way beyond the specified range of 0.3 to 0.7 gpm.

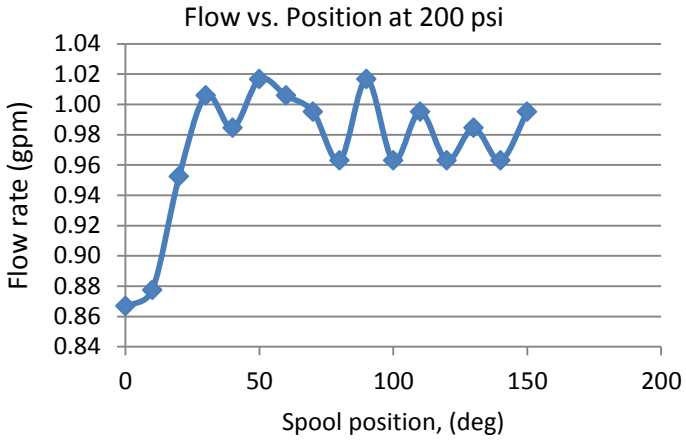

Figure D2. Flow vs spool rotation at 200psi.

Conclusion

In its current state, there is too much leakage in this prototype valve to be suitable for use as a proportional valve. At 200 psi the valve allowed more fluid to pass in its closed configuration than the specified flow for the knee mechanism. While this remains a potentially attractive solution to the problem, given limited time and resources this option is beyond the scope of this research project.